Title

Liénard-Wiechert Numerical Radiation Modeling for Plasma Acceleration Experiments at FACET-II

Authors

Yadav, M
Hansel, C
Majernik, N
et al.

Publication Date

2021

DOI

10.18429/JACoW-IPAC2021-MOPAB148

ISBN: 978-3-95450-214-1 ISSN: 2673-5490 doi:10.18429/JACoW-IPAC2021-MOPAB148

LIÉNARD-WIECHERT NUMERICAL RADIATION MODELING FOR PLASMA ACCELERATION EXPERIMENTS AT FACET-II

M. Yadav*[1,2], C. Hansel†, N. Majernik, P. Manwani, Y. Zhuang, G. Andonian, O. Williams, B. Naranjo, J. B. Rosenzweig, University of California, Los Angeles, CA, USA, 90095, USA
A. Perera, O. Apsimon, C. P. Welsch[2], University of Liverpool, Liverpool, L69 3BX, United Kingdom
[1] also at University of Liverpool, Liverpool, L69 3BX, United Kingdom
[2] also at Cockcroft Institute, Warrington WA4 4AD, United Kingdom

Abstract

Planned plasma acceleration experiments at FACET-II will use betatron radiation emitted by both the drive and witness beams to provide single shot non-destructive beam diagnostics. We numerically model this radiation by computing the Liénard-Wiechert fields from the trajectories of particles tracked by the Quasi-Static Particle-in-Cell (PIC) QuickPIC. This model is validated against analytical expressions and the radiation for a prototypical FACET-II plasma acceleration experiment is discussed. Finally, we calculate the radiation signature produced by witness beams of different spot sizes and discuss the implications on betatron radiation diagnostics at FACET-II.

INTRODUCTION

The Facility for Advanced Experimental Tests II (FACET-II) [1, 2] is a test facility at SLAC National Accelerator Laboratory primarily dedicated to research and development of advanced acceleration technologies. FACET-II has a number of ambitious research goals which require the measurement of low emittance beams including the demonstration of emittance preservation in a plasma accelerator, the creation of ultra high brightness beams from a plasma photocathode. Achieving these goals requires sophisticated beam diagnostics. The utility of betatron radiation diagnostics has already proven in inverse compton scattering experiments [3]. Betatron radiation encodes a wealth of information about ultrafast relativistic beam-plasma interactions. In this paper we first discuss a numerical model for this radiation which is validated against analytical theory. Next, we show the properties of the betatron radiation from a prototype simulation with FACET-II relevant parameters. The witness beam spot size of this prototype simulation is varied, and the effects on the radiation spectrum and angular distribution are shown. Finally, we discuss concerns related to the realization of betatron radiation diagnostics at FACET-II.

ANALYTICAL RADIATION SPECTRUM

In a blowout regime plasma accelerator, the uniform ion distribution inside the bubble generates a linear transverse electric field which focuses the witness beam [4]. The particles inside the bubble undergo simple harmonic transverse betatron oscillations which produces betatron radiation [5, 6]. This radiation is analogous to that produced in a wiggler with undulator parameter $K = k_p a\sqrt{\gamma/2} \gg 1$ where $k_p = \sqrt{4\pi r_e n_0}$ is the plasma angular wavenumber, a is the amplitude of the betatron oscillation, n_0 is the plasma density, and r_e is the classical electron radius. However in contrast to a wiggler where the beam is offset from the axis and each particle has roughly the same K, a beam in a plasma accelerator is in most cases centered on the axis and each particle has a different value of K. For a single particle, the radiation spectrum is given by [7]

$$\left(\frac{dI}{d\epsilon}\right)_s = \frac{I_{0,s}}{\epsilon_{c,s}} S_s\left(\frac{\epsilon}{\epsilon_{c,s}}\right) \tag{1}$$

where $I_{0,s} = r_e m_e c^2 k_p^4 L_p \gamma^2 a^2/12$ is the total radiated energy, $\epsilon_{c,s} = 3\hbar c k_p^2 \gamma^2 a/4$ is the critical energy, and $S(x)$ is the universal function of synchrotron radiation

$$S_s(x) = \frac{9\sqrt{3}}{8\pi} x \int_x^\infty K_{5/3}(y)dy \tag{2}$$

which satisfies the normalization condition $\int_0^\infty S_s(x)dx = 1$. The betatron radiation for a zero-emittance, monochromatic, transversely symmetric, Gaussian electron beam can be obtained by integrating the single particle spectrum over a range of the betatron amplitudes, a, in the beam as in

$$\begin{aligned}\left(\frac{dI}{d\epsilon}\right)_b &= 2\pi \int_0^\infty \left(\frac{dI}{d\epsilon}\right)_s \frac{Q}{2\pi\sigma_\perp^2 e} e^{-\frac{a^2}{2\sigma_\perp^2}} a da \\ &= \frac{I_{0,b}}{\epsilon_{c,b}} S_b\left(\frac{\epsilon}{\epsilon_{c,b}}\right)\end{aligned} \tag{3}$$

where $I_{0,b} = r_e m_e c^2 k_p^4 Q L_p \gamma^2 \sigma_\perp^2/6e$ is the total radiated energy, $\epsilon_{c,b} = 3\hbar c k_p^2 \gamma^2 \sigma_\perp/4$ is the critical energy, and $S_b(x)$ is the function

$$S_b(x) = \frac{9\sqrt{3}}{16\pi} x^3 \int_0^\infty \int_v^\infty \frac{K_{5/3}(u) e^{-\frac{x^2}{2v^2}}}{v^3} du dv \tag{4}$$

normalized such that $\int_0^\infty S_b(x)dx = 1$. A plot of the functions $S_s(x)$ and $S_b(x)$ is shown in Fig. 1.

* monika.yadav@liverpool.ac.uk
† clairehansel3@gmail.com,

ISBN: 978-3-95450-214-1 ISSN: 2673-5490 doi:10.18429/JACoW-IPAC2021-MOPAB148

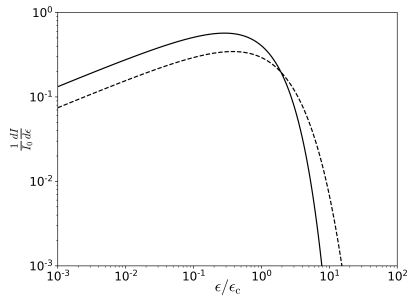

Figure 1: Normalized analytic betatron radiation spectra as functions of the normalized radiation energy. Solid Line: Single particle spectrum $S_s(\epsilon/\epsilon_c)$ given by Eq. (2). Dashed Line: Beam spectrum $S_b(\epsilon/\epsilon_c)$ given by Eq. (4). Note that both spectra are normalized to the same critical energy $\epsilon_c = \epsilon_{c,s} = \epsilon_{c,b}$ which implies that the single particle spectrum shown is for a particle with amplitude a equal to the beam spot size $\sigma_\perp$.

QUASI-STATIC PARTICLE-IN-CELL WITH LIÉNARD-WIECHERT RADIATION

In order to efficiently and accurately model betatron radiation, we used a method similar to [8]. We modified the Quasi-Static Particle-In-Cell (PIC) code `QuickPIC` [9, 10] to output particle trajectories. We developed a code which takes these trajectories as its input and computes the radiation by numerically integrating the Liénard–Wiechert integral as given in Eqs. (5) and (6) [7]

$$V_i = \int_{t_i}^{t_f} \frac{\hat{n} \times ((\hat{n} - \beta(t)) \times \dot{\beta}(t))}{(1 - \hat{n} \cdot \beta(t))^2} e^{i\omega(t - \hat{n}\cdot r(t)/c)} dt \quad (5)$$

$$\frac{d^2I}{d\Omega d\epsilon} = \frac{e^2}{16\pi^3 \epsilon_0 \hbar c} \left| \sum_i V_i \right|^2 . \quad (6)$$

where $\hat{\mathbf{n}}$ is the direction unit vector radiation is measured in, $\mathbf{r}$ is the position vector of the particle, and is the particle velocity vector normalized to c, and $\omega = \epsilon/\hbar$.

Table 1: Parameters Used to Benchmark PIC + LW Code

Parameter	Value	Unit
Plasma		
n_0	4×10^{16}	cm^{-3}
L_p	60	cm
r_p	31.88	μm
Drive/Witness Beam		
Q	500/10	pC
E	10/10	GeV
$\sigma_{x,y,z}$	5/2	μm
$\epsilon_{nx,ny}$	3/14.89	μm
ξ_0	102	μm

Computing radiation from all of the trajectories output by the PIC code is computationally infeasible and so a subset is randomly sampled and the final result is scaled. Accurate modeling of high frequency radiation requires a smaller step size, dt in Eq. (5), than the step size required to accurately track particles in the PIC code. Therefore, a cubic B-spline interpolation was used to increase the number of points in each particle trajectory exported from the PIC code. In order to validate the PIC+LW code, a simulation was run with the parameters shown in Table 1. Longitudinal acceleration of the witness beam, which is not accounted for in the analytic expression given by Eq. (3), was minimized through the use of a narrow plasma and a witness beam in a judiciously chosen z position. The computed spectrum, shown in Fig. 2, is is very good agreement with the analytical expression Eq. (3). Despite the many advantages of this PIC+LW code, it has a number of limitations including an inability to model beam energy loss due to radiation.

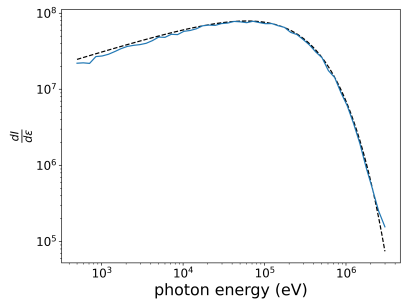

Figure 2: Blue: Radiation spectrum computed numerically using the PIC+LW code. Black, Dashed: Analytical radiation spectrum given by Eq. (3).

PRELIMINARY SIMULATIONS

We characterized the radiation for a prototypical parameter set based on what is feasible for plasma wakefield acceleration experiments at FACET-II. These parameters are shown in Table 2. The spectrum of radiation produced by the drive, witness, and both beams are shown in Fig. 3. The noise in the spectrum is primarily a result of the finite ϕ_x/ϕ_y step size. It is clear that the lion's share of the radiation is produced by the drive beam, which means diagnosing witness beam parameters is challenging as variation in the witness beam spectrum will have a relatively small effect on the overall radiation. This is discussed further in the conclusion.

WITNESS SPOT SIZE SCAN

Reconstruction of the beam parameters from the radiation signature requires an understanding of how the parameters of the beam affect the radiation produced in the beam-plasma interaction. The prototypical parameter set was perturbed in a number of ways. The full results will be presented in a future publication [11]. Here we show the result of a parameter scan over the initial witness beam spot size. The

ISBN: 978-3-95450-214-1 ISSN: 2673-5490 doi:10.18429/JACoW-IPAC2021-MOPAB148

Table 2: Prototype Simulation Parameters

Parameter	Value	Unit
Plasma		
n_0	1.79×10^{16}	cm^{-3}
L_p	30	cm
L_{ramp}	10	cm
σ_{ramp}	$3.3\overline{3}$	cm
Drive/Witness Beam		
Q	1.5/0.5	nC
E	10/10	GeV
$\sigma_{x,y}$	5/4.5	μm
σ_z	30/12.15	μm
$\epsilon_{nx,ny}$	5/5	μm
ξ_0	180	μm

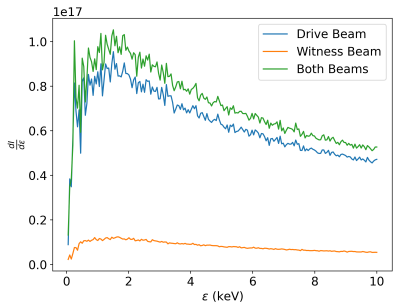

Figure 3: Betatron radiation spectrum from the prototype simulation.

evolution of the witness beam spot size over the length of the plasma is shown in Fig. 4. The *witness beam* spectra and 1-D angular distributions are shown in Fig. 5. These results show that, except for the $\sigma_i = 2.5\,\mu m$ case which, as can be seen in Fig. 4 is somewhat overfocused, larger initial spot sizes lead to more radiation and a wider angular distribution.

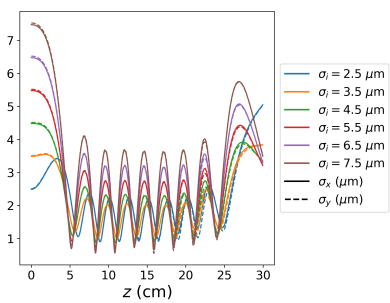

Figure 4: Evolution of witness beam spot size throughout the length of the plasma.

The main goal of this research is to be able to diagnose the parameters of a beam from the spectral and angular distribution of the betatron radiation which encodes information about the beam-plasma interaction.

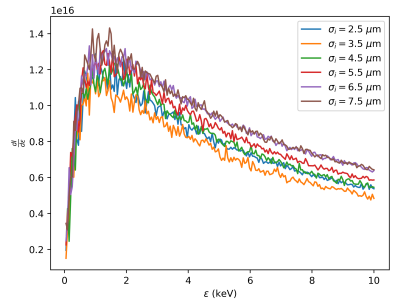

(a)

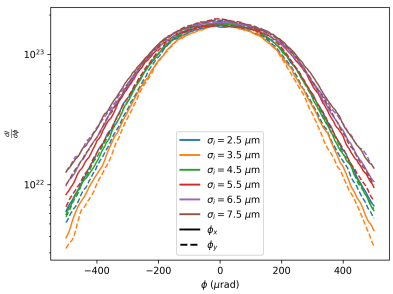

(b)

Figure 5: (a): Spectra of radiation generated by witness beam for a range of different initial spot sizes. (b): 1D angular distribution of betatron radiation generated by witness beam for a range of different initial spot sizes.

CONCLUSION

Above we have discussed betatron radiation diagnostics modeling for FACET-II. We described the design of a PIC+LW code for betatron radiation modeling. This model is more efficient than other approaches such as full PIC codes with Liénard-Wiechert or QED radiation models. We validated our code against analytic expressions. We presented simulations of the betatron radiation for FACET-II relevant parameters including a scan over different witness beam spot sizes.

Diagnosing witness beam parameters from betatron radiation is challenging in cases where the majority of the radiation is being produced by the drive beam. This may present challenges for some experiments at FACET-II. However, because the total radiation emitted by a beam scales as $I_{b,0} \sim Q\gamma^2\sigma_\perp^2$, this is less of an issue for witness beams that have higher charges, larger spot sizes, or higher energies.

ACKNOWLEDGEMENT

This work was performed with support of the US Department of Energy, Division of High Energy Physics, under Contract No. DE-SC0009914, and the STFC Liverpool Centre for Doctoral Training on Data Intensive Science (LIV.DAT) under grant agreement ST/P006752/1.

ISBN: 978-3-95450-214-1 ISSN: 2673-5490 doi:10.18429/JACoW-IPAC2021-MOPAB148

REFERENCES

[1] V. Yakimenko, *et al.*, "FACET-II facility for advanced accelerator experimental tests", *Phys. Rev. Accel. Beams*, vol. 22, no. 10, p. 101301, Oct. 2019. doi:10.1103/PhysRevAccelBeams.22.101301

[2] C. Joshi *et al.*, "Plasma wakefield acceleration experiments at FACET II", *Plasma Phys. Controlled Fusion*, vol. 60, no. 3, p. 034001, Jan. 2018. doi:10.1088/1361-6587/aaa2e3

[3] Y. Sakai *et al.*, "Single shot, double differential spectral measurements of inverse Compton scattering in the nonlinear regime", *Phys. Rev. Accel. Beams*, vol. 20, no. 6, p. 060701, Jun. 2017. doi:10.1103/PhysRevAccelBeams.20.060701

[4] J. B. Rosenzweig *et al.*, "Acceleration and focusing of electrons in two-dimensional nonlinear plasma wake fields", *Phys. Rev. A*, vol. 44, no. 10, pp. R6189–R6192, Nov. 1991. doi:10.1103/PhysRevA.44.R6189

[5] E. Esarey *et al.*, "Synchrotron radiation from electron beams in plasma-focusing channels", *Phys. Rev. E*, vol. 65, no. 5, p. 05605, May 2002. doi:10.1103/PhysRevE.65.056505

[6] S. Corde *et al.*, "Femtosecond x rays from laser-plasma accelerators", *Rev. Mod. Phys.*, vol. 85, no. 1, pp. 1–48, Jan. 2013. doi:10.1103/RevModPhys.85.1

[7] A. Hofmann, *The Physics of Synchrotron Radiation*, Cambridge, MA, USA: 2004.

[8] P. S. M. Claveria *et al.*, "Betatron radiation and emittance growth in plasma wakefield accelerators", *Philos. Trans. R. Soc. London, Ser. A*, vol. 377, no. 2151, p. 20180173, Jun. 2019. doi:10.1098/rsta.2018.0173

[9] W. An *et al.*, "An improved iteration loop for the three dimensional quasi-static particle-in-cell algorithm: QuickPIC", *J. Comput. Phys.*, vol. 250, pp. 165–177, Oct. 2013. doi:10.1016/j.jcp.2013.05.020

[10] C. Huang *et al.*, "QUICKPIC: A highly efficient particle-in-cell code for modeling wakefield acceleration in plasmas", *J. Comput. Phys.*, vol. 217. no. 2, pp. 658–679, Sep. 2006. doi:10.1016/j.jcp.2006.01.039

[11] M. Yadav *et al.*, "Numerical Modeling of Betatron Radiation for Beam-Plasma Interaction Diagnostics at FACET-II", *Phys. Rev. Accel. Beams*, in preparation.